SILICA COATED CELLULOSE NANOCRYSTALS AS ADDITIVES FOR POLYMER NANOCOMPOSITES

Nicole C. Jankovic[1], David Antoniuk[2] and Mark T. McDermott[3]

[1] Department of Chemistry, University of Alberta, Edmonton, AB, Canada T6G 2G2,
njankovi@ualberta.ca, njankovic@aqmaterials.com
[2] Applied Quantum Materials Inc., 2011 94 Street, Edmonton, AB, T6N 1H1,
dantoniuk@aqmaterials.com, www.aqmaterials.com
[3] Department of Chemistry, University of Alberta, Edmonton, AB, Canada T6G 2G2,
mark.mcdermott@ualberta.ca, mcdermottgroup.wordpress.com

Keywords: Silica, Cellulose Nanocrystals, Nanorods, Nanocomposites

ABSTRACT

Cellulose nanocrystals (CNCs) have become an attractive bio-based and bio-degradable alternative to common composite fillers, such as glass fibres and carbon nanotubes. However, due to the low temperature stability of CNC and the hydrophilic hydroxyl rich surface, processing into polymer composites has proven challenging. This is especially pertinent for incorporation into industrially relevant hydrophobic polymers such as high or low density polyethylenes, polystyrenes, and rubber. Thus, this study reports the tailorable in-situ coating of CNC with silica. TEM imaging reveals a "bead on a string" type structure, with the silica forming as a beaded coating on CNC. The final silica coated CNCs (SiO_2-CNC) also show improved thermal stability up to 300˚C and increased dispersibility in organic solvents, such as toluene. Further, preliminary mechanical tests in thermoplastic polyurethane (TPU) were performed. The SiO_2-CNC nanoparticles described here combines the excellent mechanical properties of CNC with the enhanced matrix-filler interactions provided by silica, making it an easy high-strength replacement for the silica microparticles already used in industry.

1 INTRODUCTION

Interest in cellulose nanomaterials has grown considerably over the past few decades due to its appeal as a reinforcing filler that is renewable and biodegradable.[1] Specifically, cellulose nanocrystals (CNCs) have been widely used in polymer composites as they have been shown to increase composite mechanical properties, such as elastic modulus, at very low loadings (*i.e.,* sub 5 wt%).[2] These significant improvements in composite properties achieved at low loadings are due to the nanometer size and low density of CNC. However, CNCs are hydrophilic, which make composite mixing into industrially relevant polymers, such as rubbers or polyethylenes, difficult.[3] Thus, surface modifications are typically performed to enhance matrix-filler interactions.[4, 5]

A suite of modifications has been reported in the literature for the improved incorporation of CNC in polymer matrices.[6, 7] However, most of the previous studies focused on modifying the CNC surface with monomers of the polymer matrix using complicated synthetic procedures. Contrary to CNCs, silica (SiO_2) has been one of the most widely used composite fillers, ranging from applications in cosmetics to tire compositions. Little to no modification of the silica surface is done when incorporating silica into these matrices, suggesting a strong interaction between the silica surface and the polymer.[8] Silica microparticles are already currently being used in polymer materials for increased strength, thus the addition of the rod-shaped CNC nanoparticles can introduce unique anisotropic mechanical properties.[9] By harnessing the mechanical advantage of CNC and silica, alongside the compatibilization of silica in hydrophobic polymers, the possibility for advanced functional materials is extensive. Coatings, therefore, are crucial for the incorporation of the high tensile strength CNC particles in industrially relevant polymers.

Our hypothesis is that coating CNCs with a thin layer of silica will increase compatibilization in polymer composites, and the combined advantageous properties of both CNC and silica will result in interesting, high-performance materials. The research presented here utilizes CNC as a rod-shaped, hard template for silica coating *via* a layer-by-layer (LbL) approach in a one-pot reaction performed at ambient conditions. TEOS, or tetraethyl orthosilicate, was used for the formation of a more hydrophobic silica coating on CNC. The thickness of the nanoparticles was controlled by adjusting the amount of silica source added. The coating was characterized using TEM and FTIR, and the thermal stability was measured using TGA. Preliminary results show that the CNC core provides mechanical reinforcement while the addition of silica changes the surface chemistry of the CNCs. This causes an increase in interactions with otherwise incompatible polymers, such as elastomers and other hydrophobic polymers.

2 MATERIALS AND METHODS

Spray-dried sulfate half ester Na-form cellulose nanocrystals (Batch COMP181121-H) were purchased from Innotech Alberta (Edmonton, AB, CA). Polydiallyldimethylammonium chloride (PDDA) 20wt% in H_2O, 28-30% ammonium hydroxide solution, and 98% tetraethyl orthosilicate (TEOS) was purchased from Millipore Sigma (Oakville, ON, CA). Ethanol (70%) was purchased from Fisher Scientific Canada. Anhydrous ethanol was purchased from Greenfield Global (Irvine, CA, USA). Distilled water was used in all cases of water. All materials were used as received.

The synthesis of the silica coated cellulose nanocrystals was adapted from Chen et al.[10] The synthesis started with the addition of CNC (1 g) to distilled water (42 mL) while stirring. Next, PDDA (3.3 mL) was added and allowed to stir overnight. The solution was diluted with 268 mL of 70% ethanol and 22 mL of anhydrous ethanol. Ammonium hydroxide (4.6 mL) was added followed by the dropwise addition of TEOS (1, 2, 3, 6, and 12 mL). The solution was stirred overnight. The solution was left to settle, solvent was decanted, and the final slurry was centrifuged three times in water. The silica coated CNCs were freeze dried from water to obtain a dried white powder. Table 1 lists each sample code and the relative amounts of CNC and TEOS added. Sample codes were named after the amount of TEOS added.

Sample Code	**Mass$_{CNC}$ (g)**	**Volume$_{PDDA}$ (mL)**	**Volume$_{TEOS}$ (mL)**
SiO_2-CNC-1	1	3.3	1
SiO_2-CNC-2	1	3.3	2
SiO_2-CNC-3	1	3.3	3
SiO_2-CNC-6	1	3.3	6
SiO_2-CNC-12	1	3.3	12

Table 1: Sample codes and compositions for the SiO_2-CNC nanorods.

Fourier transform infrared (FTIR) analysis was completed using an IRSpirit spectrophotometer (Shimazdu; Kyoto, JP). Freeze dried samples were placed onto the Ge crystal and 60 scans were run between 700 and 4000 cm^{-1} with a resolution of 2. A background scan was collected before each spectrum. Transmission electron microscopy (TEM) images were collected using a JEOL JEM-ARM200CF S/TEM (Narwhal) microscope. Small amounts of freeze-dried samples were dispersed in ethanol, sonicated for 30min, then drop-casted onto a 300 copper mesh TEM grid with ultra-thin carbon coating. Thermogravimetric analysis (TGA) was performed using a Perkin Elmer Pyris 1 TGA instrument. All samples were heated from room temperature (~25˚C) to 700˚C at a heating rate of 10˚C/min and using argon as the carrier gas.

Spin coated samples for tensile testing were prepared by first dissolving the SiO_2-CNC powder in dimethylformamide (DMF), sonicating 30 minutes, adding the TPU pellets, and finally stirring at 45˚C until dissolved. The total CNC+TPU in DMF was 20 wt/v% and the loadings used of the silica CNCs compared to TPU was 0, 0.5, 1, and 2.5 wt/wt%. Next, 2mL of each sample was spin coated onto cleaned glass microscope slides at 1000 rpm for 60 seconds. The dried films were peeled of the glass substrate, and strips were cut down the middle with dimensions of 10 mm (width) by 75 mm (length) and stored in a desiccator until used for tensile testing. Mechanical tests were performed using a TA Instruments ElectroForce 3200 uniaxial testing machine (450 N max. capacity load cell). A C-shaped frame made from paper was used to hold the samples in the grips to prevent sliding. The gauge length was set to 50 mm and the strain rate used was 0.1mm/s.

3 RESULTS AND DISCUSSION

The coating of CNC with silica was controlled by varying the amount of TEOS, as shown in Table 1. The PDDA binds electrostatically to the negatively charged CNC creating a surface with net positive charge that acts as a favourable interface for the formation of silica seeds for bead growth. A general reaction scheme for the synthesis is presented in Figure 1.

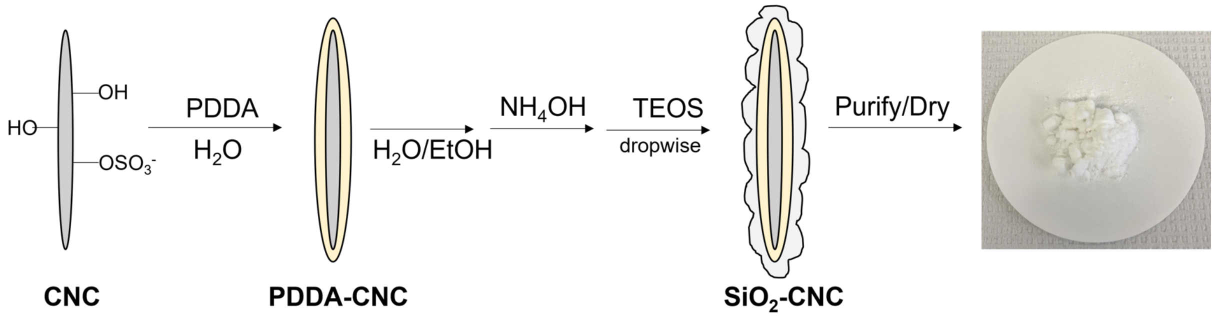

Figure 1: Schematic outlining the general reaction scheme for the coating of CNC with silica.

The thickness of the silica layer is evaluated using TEM, as shown in Figure 2. Both the SiO_2-CNC-1 and SiO_2-CNC-2 samples in Fig. 2A and 2B, respectively, show thin rods with little to no coating. These samples more closely resembled polymer coated CNCs. As the concentration of TEOS was increased, so did the thickness of the silica layer, as seen for the higher concentration samples in Fig. 2C-E. In addition, the SiO_2-CNC-6 and -12 samples show more variability in the particle size as some particles had thinner coatings and some particles had larger thicker coatings. Figure 2F shows the silica bead diameter on the CNC surface as a function of TEOS concentration. The SiO_2-CNC-3 sample shows the least variability in bead diameter whereas the SiO_2-CNC-12 sample shows the most variability and a higher average bead diameter. The common explanation for the growth of silica spheres is described using Ostwald ripening – where at high concentrations, larger particles are kinetically favoured and become larger while smaller particles become smaller and dissolve more readily.[11] This may explain why the high TEOS samples have larger variability and thus less control in the uniformity of the coating. The most uniform silica coating observed in this study is in the SiO_2-CNC-3 samples.

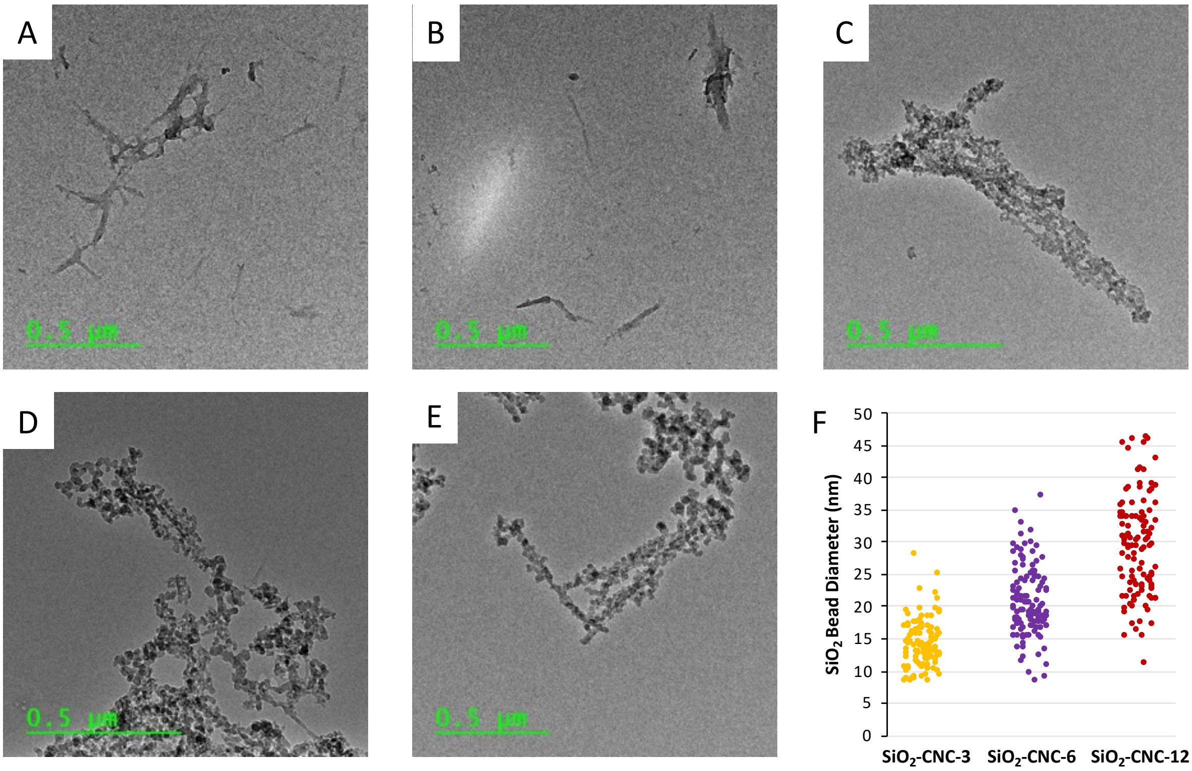

Figure 2: Bright field TEM images of: A) SiO_2-CNC-1, B) SiO_2-CNC-2, C) SiO_2-CNC-3, D) SiO_2-CNC-6, E) SiO_2-CNC-12, and F) jitter plot showing silica bead diameter.

The chemical structure of the SiO_2-CNC nanoparticles is revealed in the infrared spectra shown in Figure 3. At lower TEOS concentrations (SiO_2-CNC-1 and 2), the FTIR more closely resembles that of unmodified CNC.[12] As concentration increased, a strong Si-O stretch appears in SiO_2-CNC-3 at around 1050 cm^{-1} while the C-O characteristic peaks of CNC from 970-1170 cm^{-1} become covered by the strong silica peak. The area under this peak also appears to become larger with increasing concentration. The findings from FTIR are consistent with TEM, as a thicker silica coating suggests more silica is present in the samples. The SiO_2-CNC-6 sample show a larger presence of water, as observed with a peak at around 1600 and 3400 cm^{-1} – which is consistent with incomplete drying of the sample.

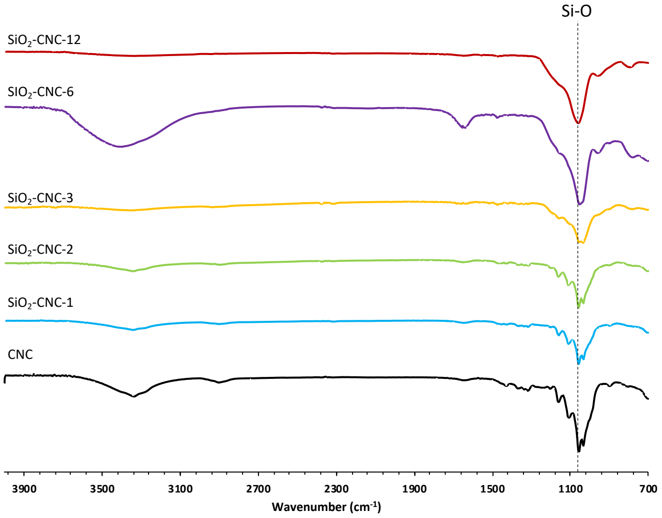

Figure 3: FTIR spectra of the SiO_2-CNCs compared to unmodified CNC (black).

A challenge in incorporating CNCs into polymers *via* thermal processing (*e.g.,* melt mixing) is the poor thermal stability of CNC. The thermal stability of the SiO_2-CNC nanoparticles is expected to be enhanced compared to CNC. Figure 4 shows both the TGA (Fig. 4A) and DTG (Fig. 4B) curves, including that of unmodified CNC. In all cases, the silica coated CNCs show a higher onset temperature (T_O) and first derivative peak temperature (T_P) when compared to unmodified CNC. Within the silica CNC samples, a higher remaining mass/char was observed with increasing TEOS concentration. Silica has a high thermal stability (think glass, for example), therefore any remaining mass is most likely due to the formation of silicon nanoparticles with some organic char.[13] As mentioned previously, SiO_2-CNC-6 is excluded in the data set as it was not fully dry thus providing inconsistent data; however, based on the trends seen in Figure 4, it is expected that this sample would fall between SiO_2-CNC-3 and SiO_2-CNC-12 when fully dried.

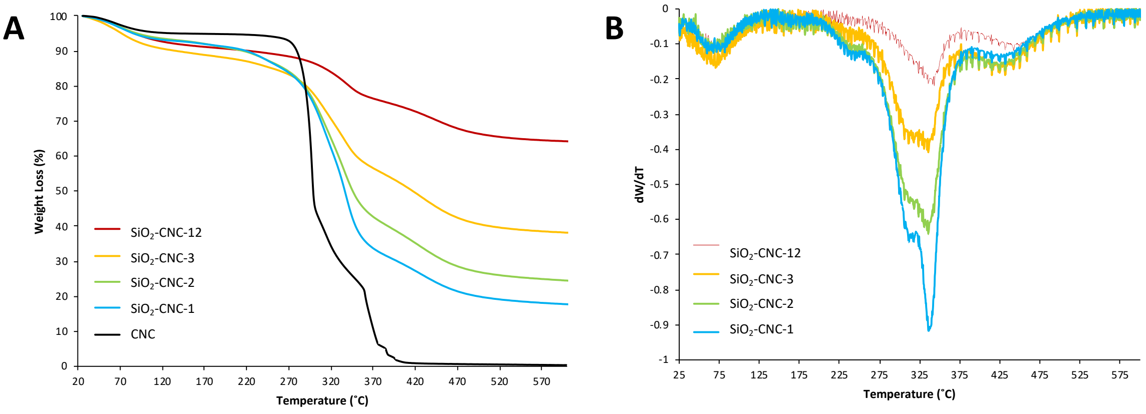

Figure 4: A) TGA and B) DTG spectra of the SiO_2-CNCs.

A preliminary study on the mechanical properties of the nanorods in a polymer was performed by spin coating solutions of SiO_2-CNC and TPU into thin films. Since the SiO_2-CNC-3 sample showed the least variability in size (as shown in Fig. 2C), it was chosen for the incorporation into the TPU composite films. Figure 5A shows photographs of the solutions prior to spin coating and Figure 5B shows the films after spin coating. The TPU films show small white aggregates with increasing concentration, however, all films appeared transparent and clear suggesting the SiO_2-CNCs did not affect the crystallization of the polymer. Figure 5C shows the elastic modulus (EM) values of the spin coated films with increasing silica CNC loading. Though a slight increase (~12%) was observed, the EM values did not statistically differ between loadings. However, the trend shows that an increase in SiO_2-CNC has a positive effect on the EM, thus higher loadings will be the topic of future studies.

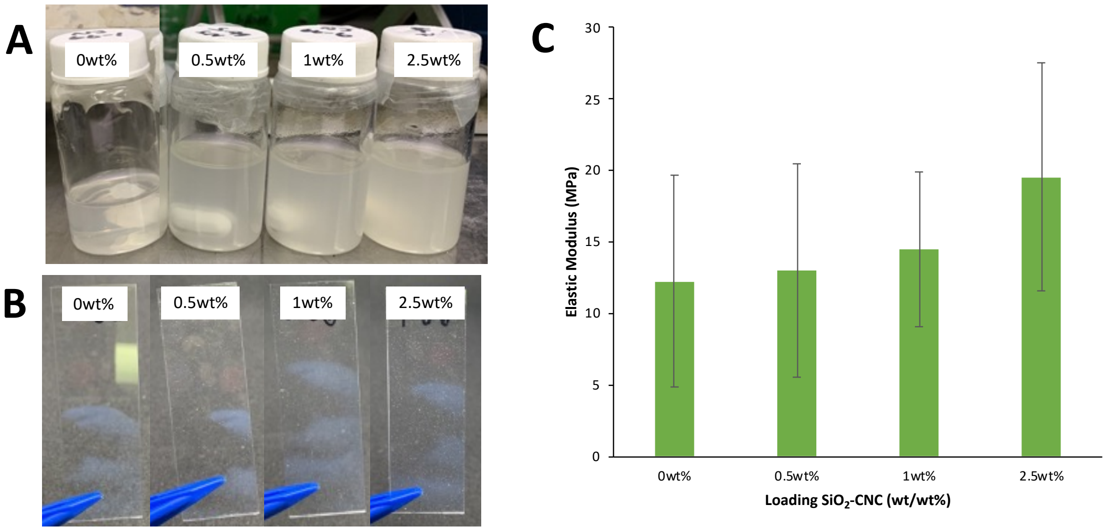

Figure 5: A) Photographs of TPU dissolved in DMF with different SiO_2-CNC-3 loadings, B) the spin coated films on the glass microscope slides, and C) the results for elastic modulus.

4 CONCLUSIONS

Silica coated cellulose nanocrystals was synthesized using a one-pot base-catalyzed reaction. The thickness of the resultant SiO_2-CNC nanorods was controllable by changing the amount of siloxane added during the reaction, as was visualized using TEM. The addition of silica increased the thermal stability up to 40˚C higher than unmodified CNC. The tensile testing results from spin coated TPU composite samples showed promise for incorporation of the SiO_2-CNCs into polymers. By adjusting the thickness of the silica nanorods, properties of numerous polymer composites can be tailored.

ACKNOWLEDGEMENTS

The authors would like to acknowledge Caoimhe Connaughton and Patricia Eiman for their assistance with the synthesis, characterization, and purification of materials. The authors also acknowledge Mitacs for financial supporting Nicole Jankovic during the project.

REFERENCES

[1] Z. Shi, S. Li, M. Li, L. Gan, and J. Huang, Surface modification of cellulose nanocrystals towards new materials development, *Journal of Applied Polymer Science,* **138**, 48, 2021, p. 51555, (doi: https://doi.org/10.1002/app.51555).

[2] S. Varshney, N. Mishra, and M. K. Gupta, Progress in nanocellulose and its polymer based composites: A review on processing, characterization, and applications, *Polymer Composites,* **42**, 8, 2021, pp. 3660-3686, (doi: https://doi.org/10.1002/pc.26090).

[3] P. Venkatraman, E. Trotto, I. Burgoyne, and E. J. Foster, Premixed cellulose nanocrystal reinforcement of polyamide 6 for melt processing, *Polymer Composites,* **41**, 10, 2020, pp. 4353-4361, (doi: https://doi.org/10.1002/pc.25717).

[4] A. Dufresne, *5. Chemical modification of nanocellulose*, Nanocellulose: From Nature to High Performance Tailored Materials, De Gruyter, 2017.

[5] S. Kalia, S. Boufi, A. Celli, and S. Kango, Nanofibrillated cellulose: surface modification and potential applications, *Colloid and Polymer Science,* **292**, 1, 2014, pp. 5-31, (doi: 10.1007/s00396-013-3112-9).

[6] C. Gomri, M. Cretin, and M. Semsarilar, Recent progress on chemical modification of cellulose nanocrystal (CNC) and its application in nanocomposite films and membranes-A comprehensive review, *Carbohydrate Polymers,* **294**, 2022, p. 119790, (doi: https://doi.org/10.1016/j.carbpol.2022.119790).

[7] S. Eyley and W. Thielemans, Surface modification of cellulose nanocrystals, *Nanoscale,* 10.1039/C4NR01756K **6**, 14, 2014, pp. 7764-7779, (doi: 10.1039/C4NR01756K).

[8] H. Zou, S. Wu, and J. Shen, Polymer/Silica Nanocomposites: Preparation, Characterization, Properties, and Applications, *Chemical Reviews,* **108**, 9, 2008, pp. 3893-3957, (doi: 10.1021/cr068035q).

[9] R. A. Chowdhury, C. Clarkson, V. A. Apalangya, S. M. N. Islam, and J. P. Youngblood, Roll-to-roll fabrication of cellulose nanocrystal-poly(vinyl alcohol) composite coatings with controlled anisotropy, *Cellulose,* **25**, 11, 2018, pp. 6547-6560, (doi: 10.1007/s10570-018-2019-5).

[10] L. Chen, R. M. Berry, and K. C. Tam, Synthesis of β-Cyclodextrin-Modified Cellulose Nanocrystals (CNCs)@Fe3O4@SiO2 Superparamagnetic Nanorods, *ACS Sustainable Chemistry & Engineering,* **2**, 4, 2014, pp. 951-958, (doi: 10.1021/sc400540f).

[11] E. Piletska *et al.*, Biomimetic Silica Nanoparticles Prepared by a Combination of Solid-Phase Imprinting and Ostwald Ripening, *Scientific Reports,* **7**, 1, 2017, p. 11537, (doi: 10.1038/s41598-017-12007-0).

[12] E. J. Foster *et al.*, Current characterization methods for cellulose nanomaterials, *Chem Soc Rev,* **47**, 8, 2018, pp. 2609-2679, (doi: 10.1039/c6cs00895j).

[13] Y.-L. Liu, W.-L. Wei, K.-Y. Hsu, and W.-H. Ho, Thermal stability of epoxy-silica hybrid materials by thermogravimetric analysis, *Thermochimica Acta,* **412**, 1, 2004, pp. 139-147, (doi: https://doi.org/10.1016/j.tca.2003.09.004).